Supplementary material

1.Experimental Section: Synthesis of RuNi@rGO, Ru@rGO and Ni@rGO

Briefly, the fresh graphene oxide 50 mg was dispersed in 5ml deionized water and sonicated for 2h. $NiCl_2 \cdot 6H_2O$ (0.06 mmol) chemicals were prepared into 10 mg/ml solution. They were stirred for 1 h until the mixture were dispersed fully. Afterward, stirring vigorously at room temperature for 12h. 150 uL $RuCl_3 \cdot 3H_2O$ was dispersed into 10 mg/mL aqueous solution and slowly added dropwise, with violently magnetically stirred for 5h. Then add saturated sodium borohydride, acting as a reducing agent to the solution and keep stirring for 5 h. After reaction, the product was collected by centrifugation, washed with deionized water several times and finally the solution was freeze-dried overnight. Before the catalytic evaluation, the as-synthesized samples were reduced in a H_2/Ar mixed gas at 700 °C (heating rate: $2^{\circ}C \cdot min^{-1}$) for 2 h, followed by cooling to the room temperature in H_2/Ar mixed gas. Moreover, the temperature was dropped to room temperature, leading to a uniformly dispersed RuNi SAA nanoparticles embedded in rGO framework. The preparation methods of pure Ru@rGO and Ni@rGO are similar to the above, except that $NiCl_2 \cdot 6H_2O$ or $RuCl_3 \cdot 3H_2O$ are not added, respectively.

2.TOF values were calculated by the following equation

The Number of catalytic active sites was calculated by the underpotential deposition of Cu (Cu-upd) method. 0.5 M H_2SO_4 + 1 mM $CuSO_4$ solution was purged by nitrogen for 20 minutes before the tests. In order to clean the working electrode (WE), i-t curves are scanned and tested at a voltage of 0.2 -0.4V in a 0.5 M H_2SO_4 solution. The Cu layer was deposited to the WE in 0.5 M H_2SO_4 +1 mM $CuSO_4$ solution, and the Cu-upd stripping voltammogram was obtained by scanning the working electrode (-0.2–0.8V vs RHE). Hence, the TOF values[1] can be calculated from LSV curve and number of Ru active sites as follows: **TOF=I/αFN**

I: I is the current (A) (the recorded current during the LSV measurements);

α: the number of electrons transferred for products formation;

F: the Faradaic constant, 96485 C mol^{-1};

N: the number of catalytic active sites (mol), the N can be calculated from the charge accumulation (Q) of Cu-UPD or H adsorption/desorption following the equation: **N=Q/2F**.

α is the number of transferred electrons corresponding to the semi-reaction that generates a molecular target product or consumes a molecular target reactant: the coefficient before the reaction equation e$^-$. Since HER is a two-electron catalytic process, α = 2.

3.Density Functional Theory Calculation

The Ni model structure was obtained from prior work.[2] In this study, the Vienna Ab Initio Simulation Package (VASP) and the projector augmented wave (PAW) method were employed to perform spin-polarized density functional theory (DFT) calculations.[3] The Perdew-Burke-Ernzerhof (PBE) functional within the generalized gradient approximation (GGA) was used to describe the electronic exchange-correlation energy.[4] A kinetic energy cutoff of 450 eV was applied. For structural optimizations and electron property calculations, the Brillouin zone was sampled using 7×7×7 and 3×3×1 k-point grids, respectively. The convergence criteria for electronic structure iterations were set to 10^{-4} eV, while the force iterations were set to 0.02 eV/Å. In the z-direction, a vacuum space larger than 15 Å was employed to prevent interactions between periodic images.

The Gibbs free energy of each elementary step can be shown in the following equation.

$$\Delta G_n = \Delta E + T\Delta S - ZPE$$

Where G is the Gibbs free energy, E is the electronic energy form DFT calculations, ZPE is zero-point energy, T is temperature of 300 K, and ΔS is the change in entropy.
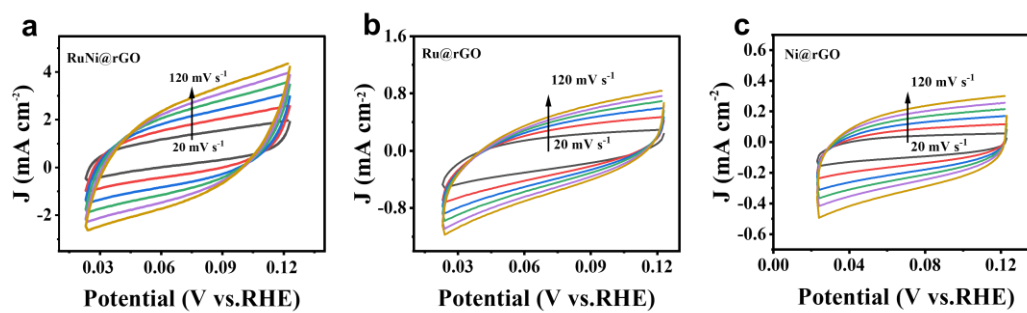
4. Supplementary Figures and Tables

Figure S1 Current difference at different scan rate for the estimation of double-layered capacitance of (a), (b) and (c) for HER in 1 M KOH.
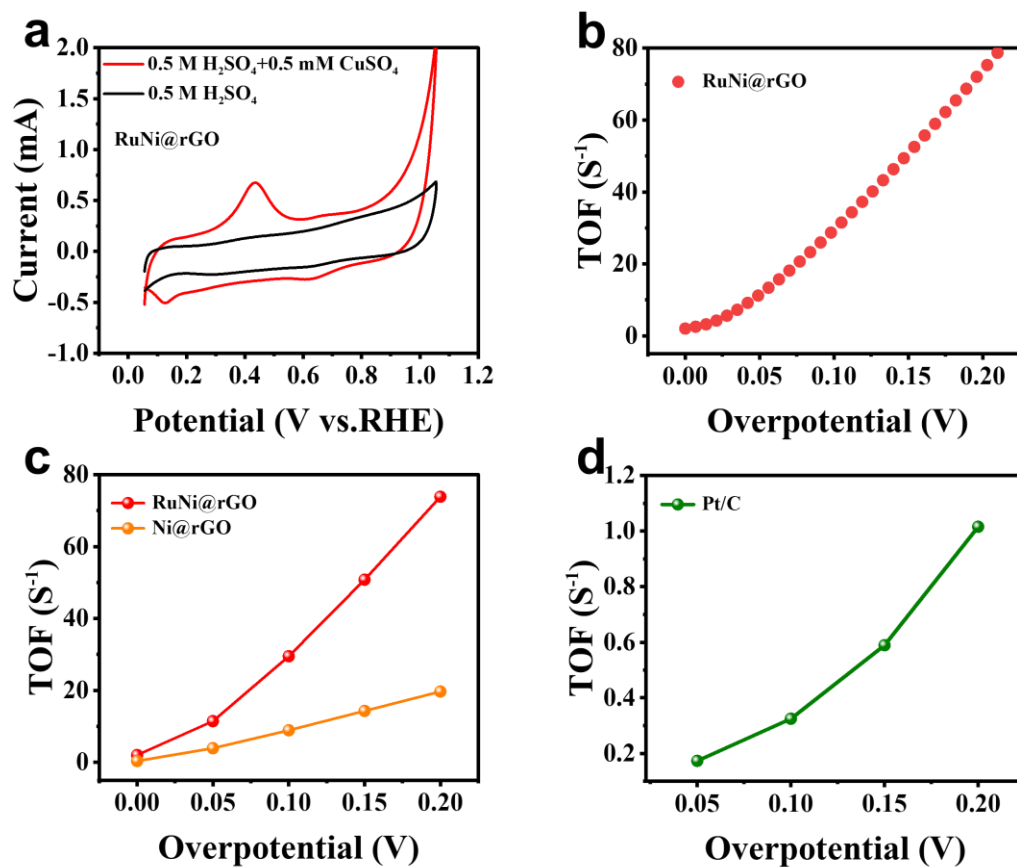
Figure S2 (a) Full range scan of Cu deposition and splitting on RuNi@rGO and Cu-upd stripping voltammogram; (b) TOFs curves of RuNi@rGO; (c and d) TOFs curves of RuNi@rGO and Ni@rGO to the HER with 20 wt% Pt/C.
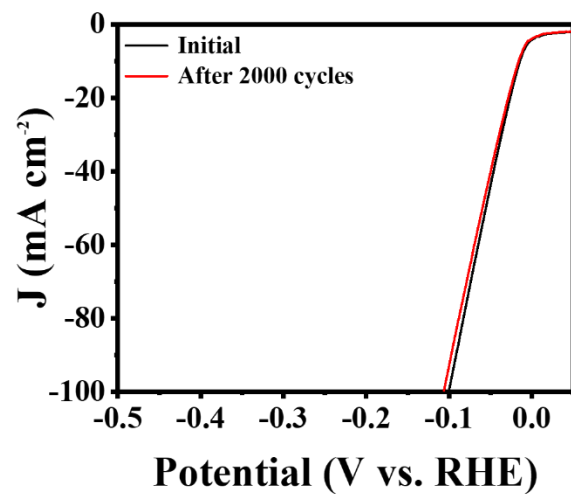
Figure S3 Comparison of the HER polarization curve of the RuNi@rGO electrocatalyst before and after 2000th cycles.
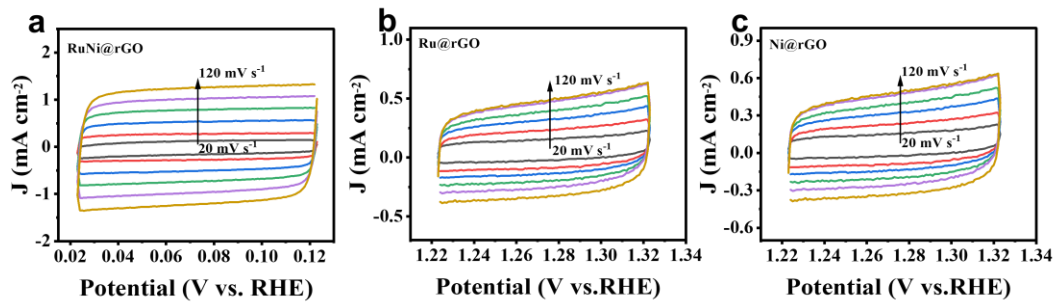
Figure S4 Current difference at different scan rate for the estimation of double-layered capacitance of (a), (b) and (c) for OER in 1 M KOH.
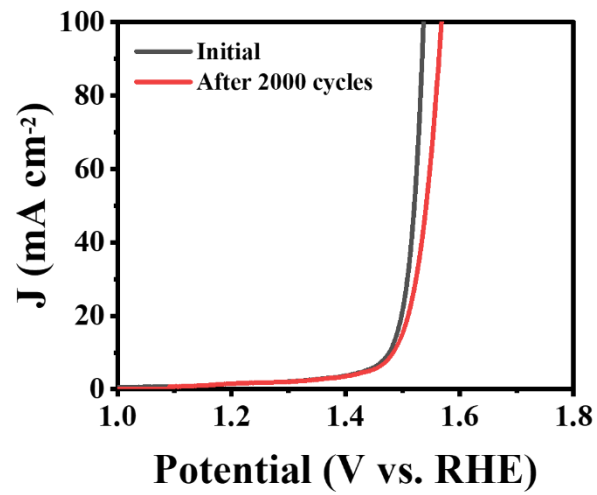
Figure S5 Comparison of the OER polarization curve of the RuNi@rGO electrocatalyst before and after 2000th cycles.
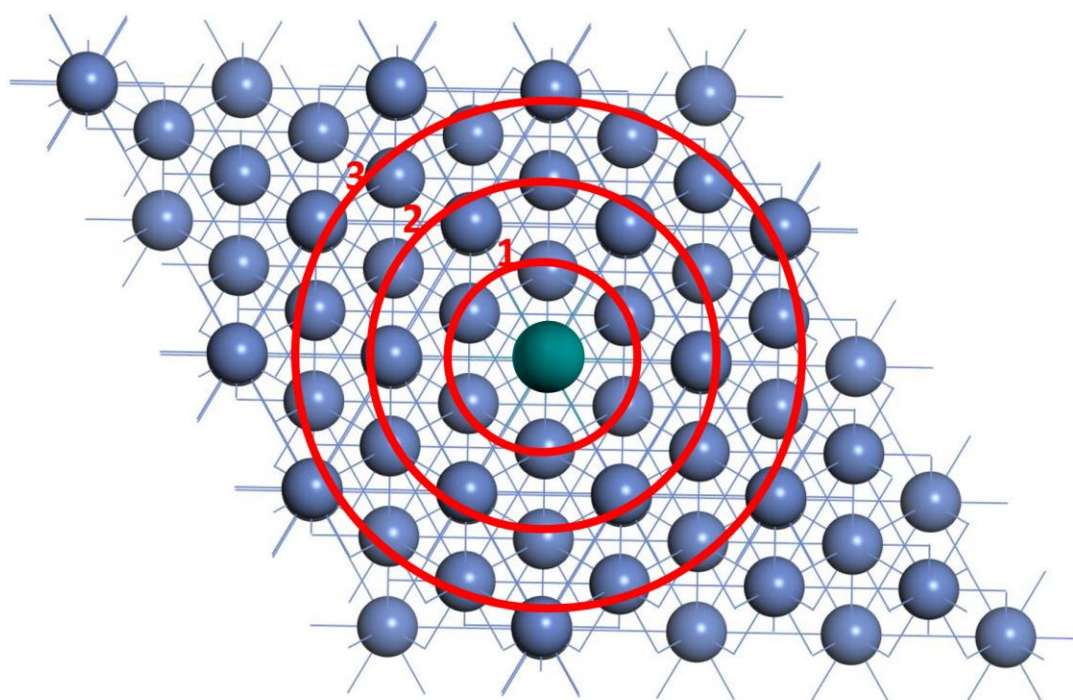
Figure S6 the structural models of three different catalytic environments on the surface of RuNi, namely RuNi -1, RuNi-2 and RuNi-3.
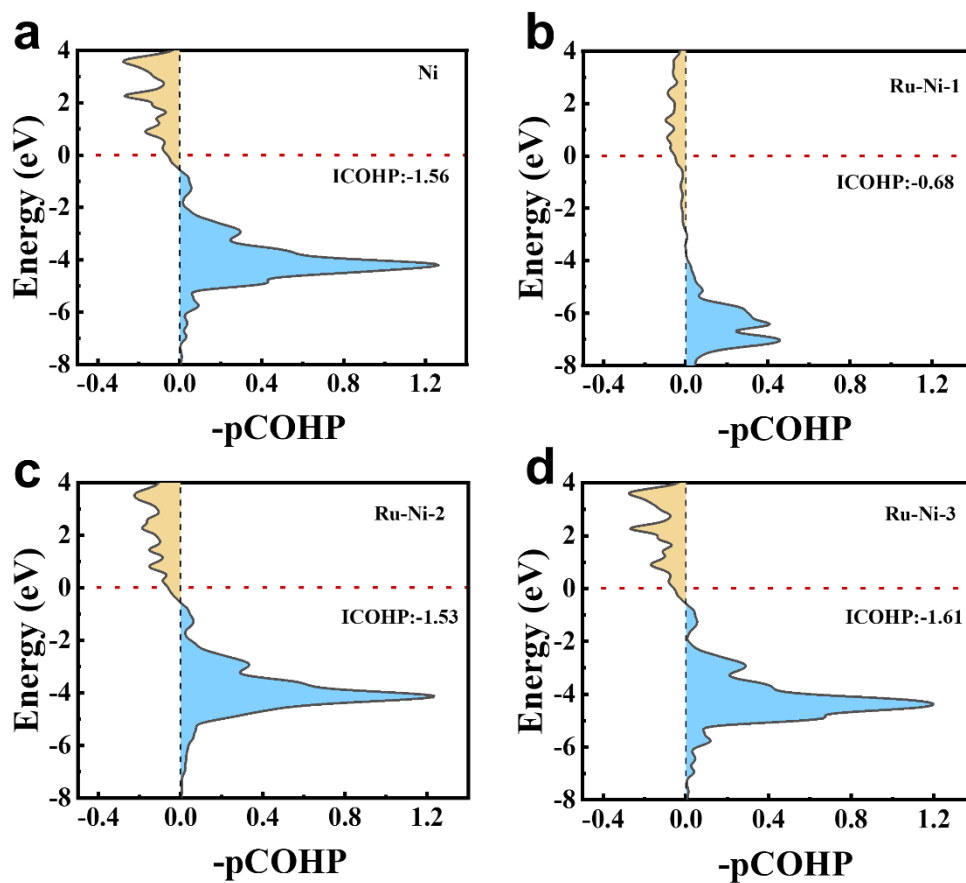
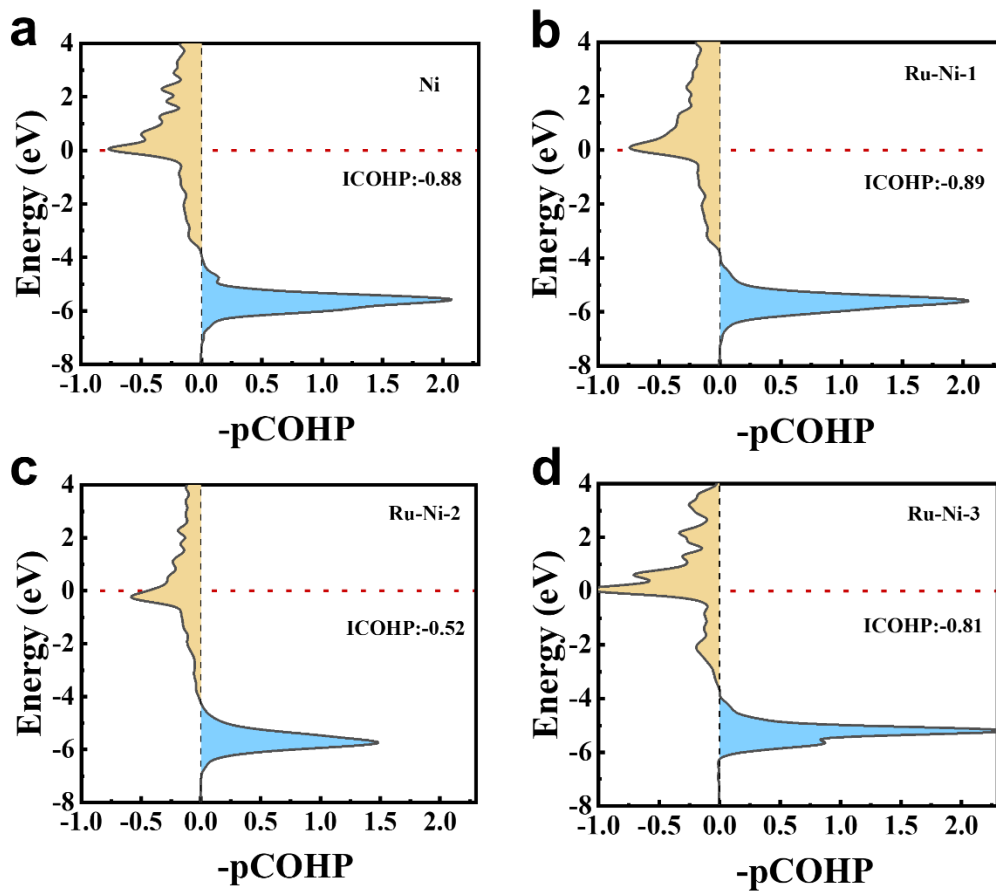**Figure S7** (a-d) The pCOHP plots of the Ni–H、RuNi-1-H、RuNi-2-H and RuNi-3-H bond in RuNi@rGO.

Figure S8 (a-d) The pCOHP plots of the Ni–O、RuNi-1-O 、RuNi-2-O and RuNi-3-O bond in RuNi@rGO.
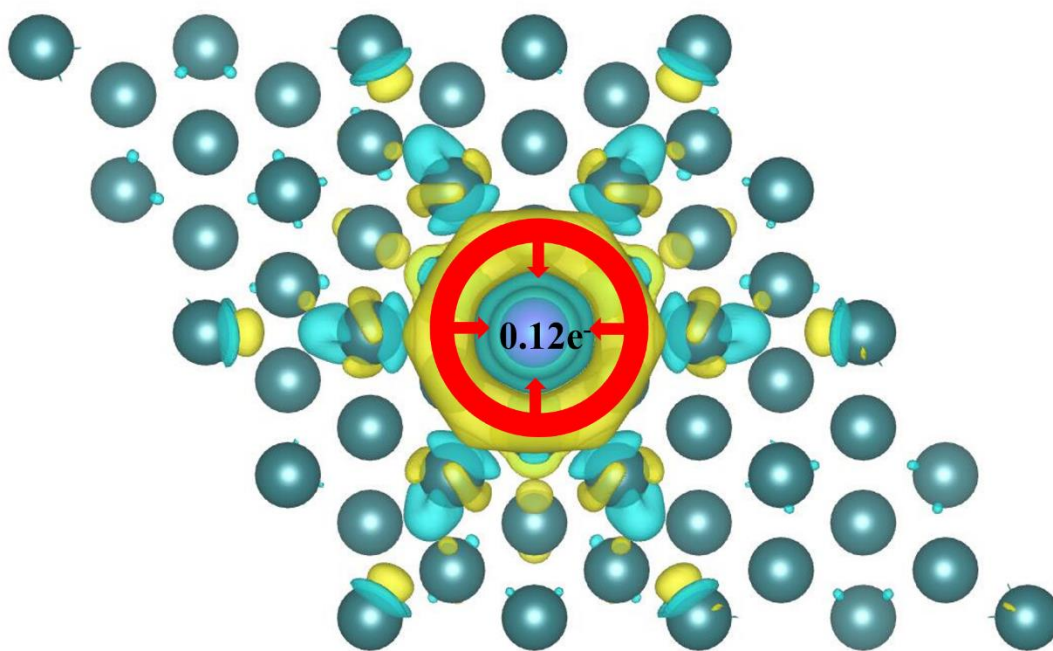
Figure S9 Differential charge density for RuNi@rGO (the ink blue and purple ball represent the Ni and Ru, respectively).

Table S1 Comparison of performance of bifunctional electrocatalysts in alkaline environments.

No.	Catalyst	HER ηj =10 (mV)	HER Tafel slop (mV dec^{-1})	OER ηj =10 (mV)	OER Tafel slop (mV dec^{-1})	Reference
1	RuNi@rGO	14	32	240	57	This work
2	RuNP@RuNx-OFC/NC	19	35.5	–	–	Appl. Catal. B., **2022**, 307, 121193.
3	Ru–Co–N–C-800 ° C	19	27.8	276	55.7	Adv. Mater. **2022**, 34, 2110103.
4	Ni$_5$P$_4$-Ru/CC	54	52	–	–	Adv. Mater. **2020**, 32, 1906972.
5	Ru/Zn$_3$V$_3$O$_8$	70	50.6	250	81.9	Nanoscale,**2021**,13,17457-17464.
6	Ru$_2$Ni$_2$ SNs/C	–	–	310	75	Nano Energy **2018**,47, 1.
7	Ru@Co/N-CNTs-2	48	33	–	–	ACS Sustainable Chem. Eng. **2020**, 8, 9136.
8	RuNi-NCNFs	–	–	290	–	Adv. Sci. **2020**, 7, 1901833.
9	Ru@NC	26	36	–	–	Angew. Chem., Int. Ed. **2018**, 57, 5848.
10	RuSx/S-GO	58	56	–	–	Small，**2019**, 15, 1904043
11	NiRu@NC	53	38	–	–	Dalton Trans., **2020**,49, 13647-13654
12	RuNi/MoC@NC	13	49.4	–	–	Nanoscale, **2023**,15, 16403-16412
13	RuNi-alloy@SC	93	96	–	–	Chemical Engineering Journal, 417 (**2021**) 129319
14	Ni$_2$P-Fe$_2$P/NF	–	–	222@100mA cm^{-2}	40.9	Sustainable Energy Fuels, **2022**,6, 4477-4483
15	Co/Ru SAs-N–C	–	–	450@100mA cm^{-2}		Catal. Sci. Technol., **2022**,12, 5435-5441
16	Ru$_2$Ni$_2$ SNs/C	–	–	310	75	Nano Energy ,**2018**,47, 1.
17	2% Ru-NCO	–	–	269@100mA cm^{-2}	–	Chemical Engineering Journal 439 (2022) 135634
18	NiCo.c	85@50mA cm^{-2}	182@50mA cm^{-2}	290@20mA cm^{-2}	149	Energy Conversion and Management, 254 (**2022**) 115262
19	ac-NiCo(OH)$_2$/NF	–	–	320@100mA cm^{-2}	–	Journal of Colloid and Interface Science, 653 (**2024**) 1704–1714

Table S2 The TOF of RuNi@rGO compared with other recently reported metal-based electrocatalysts in 1 M KOH.

No.	Catalyst	TOF (H_2 s^{-1})	Mass activity (A mg^{-1})	Reference
1	RuNi@rGO	11.45@ 50mV	29@100mV	This work
2	Ru-MoS$_2$/CC	–	0.2@169 mV	Appl. Catal. B., **2019**, 249, 91-97.
3	Pt-SAs/MoSe$_2$	6.21@ 50 mV	34.4@100 mV	Nat.Commun. **2021**,12,3021.
4	RuNP-RuSA@CFN-800	–	11.1@100 mV	Adv. Funct. Mater. **2023**, 33, 2213058.
5	Ru@C$_2$N	1.95@ 50 mV	–	Nat. Nanotech., **2017**, 12, 441–446.
6	Ru/N-C	0.7@ 50 mV	–	J. Mater. Chem. A, 2017, 5, 25314–25318.
7	PtSA/α-MoC$_{1-x}$@C	11.61@ 50 mV	26.65@100 mV	Adv. Funct. Mater. **2021**, 2108464.
8	Pt-SAs/MoSe$_2$	6.21@ 50 mV	34.4@100 mV	Nat. Commun. **2021**, 12,3021.
9	Pt-Ni ASs	18.63@ 50 mV	2.80@70 mV	Adv. Mater., **2018**,30, 1801741.

References

1 Q. He, Y. Zhou, H. Shou, X. Wang, P. Zhang, W. Xu, S. Qiao, C. Wu, H. Liu, D. Liu, S. Chen, R. Long, Z. Qi, X. Wu and L. Song, Adv. Mater, 2022, **34**, 2110604.

2 J. Liu, J. Wang, Y. Fo, B. Zhang, C. Molochas, J. Gao, W. Li, X. Cui, X. Zhou, L. Jiang and P. Tsiakaras, Chem. Eng. J, 2023, **454**, 139959.

3 G. Kresse and J. Furthmüller, Comput. Mater. Sci., 1996, **6**, 15-50.

4 Kresse and Furthmuller, Phys. Rev.,B Condens.Matter, 1996, **54**, 11169-11186.